

Broad Gap Junction Blocker Carbenoxolone Disrupts Uterine Preparation for Embryo Implantation in Mice¹

Honglu Diao,^{3,6} Shuo Xiao,^{3,4} Elizabeth W. Howerth,⁵ Fei Zhao,^{3,4} Rong Li,^{3,4} Mary B. Ard,⁵ and Xiaoqin Ye^{2,3,4}

³Department of Physiology and Pharmacology, College of Veterinary Medicine, The University of Georgia, Athens, Georgia

⁴Interdisciplinary Toxicology Program, The University of Georgia, Athens, Georgia

⁵Department of Pathology, College of Veterinary Medicine, The University of Georgia, Athens, Georgia

⁶Reproductive Medical Center, Renmin Hospital, Hubei University of Medicine, Shiyan, Hubei, China

ABSTRACT

Gap junctions have an important role in cell-to-cell communication, a process obviously required for embryo implantation. Uterine luminal epithelium (LE) is the first contact for an implanting embryo and is critical for the establishment of uterine receptivity. Microarray analysis of the LE from peri-implantation mouse uterus showed low-level expression of 19 gap junction proteins in preimplantation LE and upregulation of gap junction protein, beta 2 (GJB2, connexin 26, Cx26) in postimplantation LE. Time course study using *in situ* hybridization and immunofluorescence revealed upregulation of GJB2 in the LE surrounding the implantation site before decidualization. Similar dynamic expression of GJB2 was observed in the LE of artificially decidualized mice but not pseudopregnant mice. To determine the potential function of uterine gap junctions in embryo implantation, carbenoxolone (CBX), a broad gap junction blocker, was injected *i.p.* (100 mg/kg) or via local uterine fat pad (10 mg/kg) into pregnant mice on Gestation Day 3 at 1800 h, a few hours before embryo attachment to the LE. These CBX treatments disrupted embryo implantation, suggesting local effects of CBX in the uterus. However, *i.p.* injection of glycyrrhizic acid (100 mg/kg), which shares similar structure and multiple properties with CBX but is ineffective in blocking gap junctions, did not affect embryo implantation. Carbenoxolone also inhibited oil-induced artificial decidualization, concomitant with suppressed molecular changes and ultrastructural transformations associated with uterine preparation for embryo implantation, underscoring the adverse effect of CBX on uterine preparation for embryo implantation. These data demonstrate that uterine gap junctions are important for embryo implantation.

carbenoxolone, embryo implantation, gap junctions, uterine luminal epithelium

¹Supported by National Institutes of Health grants NIH R15HD066301 and NIH R01HD065939 to X.Y. and by funding from the Office of the Vice President for Research, Graduate School, Department of Physiology and Pharmacology, and Interdisciplinary Toxicology Program at The University of Georgia, Athens, Georgia.

²Correspondence: Xiaoqin Ye, Department of Physiology and Pharmacology, College of Veterinary Medicine, and Interdisciplinary Toxicology Program, The University of Georgia, Athens, GA 30602. E-mail: ye@uga.edu

Received: 15 April 2013.
First decision: 20 May 2013.
Accepted: 28 June 2013.
© 2013 by the Society for the Study of Reproduction, Inc.
eISSN: 1529-7268 <http://www.biolreprod.org>
ISSN: 0006-3363

INTRODUCTION

Gap junction proteins are the basic units of gap junctions, which are intercellular membrane channels connecting the cytoplasm of two neighboring cells to facilitate signal propagation [1–4]. They are widely expressed in cells, and a few of them have unique spatiotemporal expression patterns in the uterus [2, 5–10]. The most studied gap junction proteins in the uterus are GJB2/Cx26 and gap junction protein, alpha 1 (GJA1, connexin 43, Cx43). GJB2 is highly upregulated in the uterine luminal epithelium (LE) at the implantation chamber, and GJA1 is prominently localized in the decidual zone upon implantation in the rodent uterus [11–14]. GJB2 is detected in both luminal and glandular epithelial cells, and GJA1 is mainly expressed in the stromal compartment from Days 11 to 15 of the estrous cycle in the human uterus [15]. A similar expression pattern is seen in the cycling baboon, but aberrant expression of GJB2 is detected in the endometrium of the baboon model of induced endometriosis, a pathological condition associated with impaired embryo implantation [9].

Embryo implantation involves synchronized preparation of a competitive embryo and a receptive uterus [16]. Luminal epithelium is the first uterine contact for an implanting embryo, and it goes through a series of morphological changes to prepare for an embryo to implant into the uterine wall [17, 18]. Previously, we demonstrated that an LE-specific gene, *Lpar3*, the third G protein-coupled receptor for lysophosphatidic acid that is temporally regulated in the LE of peri-implantation uterus, was critical for on-time preparation of a receptive uterus in embryo implantation [19]. It was our rationale that genes with altered expression levels in the LE during peri-implantation could potentially be involved in uterine preparation for embryo implantation. Microarray analysis of Gestation Day 3.5 (D3.5) LE (preimplantation) and D4.5 LE (post-implantation) indicated that one of the gap junction proteins, *Gjb2*, was upregulated 14-fold in D4.5 LE (Gene Expression Omnibus number GSE44451). Time course *in situ* hybridization revealed upregulation of *Gjb2* in the LE at the implantation site during the initial hours of embryo implantation before decidualization became obvious. We hypothesized that *Gjb2* in the LE might have a role in embryo implantation. However, Dr. Elke Winterhager's group in Germany has not observed any obvious defect in embryo implantation in their Pax8-Cre or progesterone receptor (PR)-Cre-mediated *Gjb2* conditional knockout mice (personal communication).

As the building blocks of gap junctions, some individual gap junction proteins have been shown to have essential *in vivo* functions such as GJB2 for transplacental nutrition uptake [20], GJB2 and GJB6/Cx30 for hearing [21], and GJA1 for

decidualization and angiogenesis [22], as well as uterine contraction and parturition [23–25]. However, no individual gap junction protein has been reported to date to be essential for embryo implantation. There are 19 gap junction proteins in mice [4]. Considering the observations that one gap junction can be formed by different gap junction proteins [26], that deletion of one gap junction protein could lead to the upregulation of another gap junction protein [27], and that the function of one gap junction protein can be replaced by another gap junction protein [21], we modified our hypothesis to test the involvement of uterine gap junctions in embryo implantation using the broad gap junction blocker carbenoxolone (CBX) [5]. Because CBX has other functions such as inhibition of 11 β -hydroxysteroid dehydrogenase (11 β -HSD) and anti-inflammation [28, 29], we included glycyrrhizic acid as a control. Glycyrrhizic acid shares similar structure and multiple properties with CBX, including inhibition of 11 β -HSD [30] and anti-inflammation [28, 29], but is ineffective in blocking gap junctions [5]. This study provides novel information about gap junctions in uterine preparation for embryo implantation.

MATERIALS AND METHODS

Animals

Wild-type (WT) (C57BL6 or C57BL6/129svj mixed background), *Lpar3*^(+/-), and *Lpar3*^(-/-) mice (C57BL6/129svj mixed background) were generated and genotyped as previously described [19]. The mice were housed in polypropylene cages with free access to regular food and water from water sip tubes in a reverse osmosis system. The animal facility is on a 12L:12D cycle (light from 0600 h to 1800 h) at 23 \pm 1°C with 30%–50% relative humidity. All methods used in this study were approved by the Animal Subjects Programs of The University of Georgia and conform to National Institutes of Health guidelines and public law.

Uterine Tissue Collection

From natural pregnancy. Young virgin (2 to 4 mo old) WT and *Lpar3*^(-/-) females were mated naturally with WT stud males and checked for a vaginal plug the next morning. The day a vaginal plug was identified was designated as D0.5. Females were euthanized with CO₂ inhalation. Uterine tissues from WT females were collected on D3 at 1100 h (D3.5) and 2300 h; on D4 at 0100 h, 0400 h, 0600 h, and 1100 h (D4.5); on D5 at 1100 h (D5.5); and on D6 at 1100 h (D6.5). Uterine tissues from *Lpar3*^(-/-) females were collected on D3.5, D4.5, and D5.5.

From pseudopregnancy. Pseudopregnancy was induced by mating WT females with vasectomized WT males. Uterine tissues were collected on Pseudopregnant Day 3 at 1100 h (D3.5) and on Pseudopregnant Day 4 at 1100 h (D4.5).

From artificial decidualization. Artificial decidualization was induced as previously described [31]. Blue dye reaction [32] was determined before uterine collection on Pseudopregnant Day 3 at 2300 h (D3), on Pseudopregnant Day 4 at 0600 h (D4), and on Pseudopregnant Day 4 at 1100 h (D4.5). At least three mice were included in each time point.

CBX Treatment

Wild-type and *Lpar3*^(+/-) females, both of which have normal embryo implantation [19], were used in the pregnancy (five groups) and pseudopregnancy (two groups) studies. In the pregnancy study, the females were mated with WT stud males and randomly assigned to five groups. On D3 at 1800 h, three groups of females were injected i.p. with 100 μ l of vehicle (50% dimethyl sulfoxide in 1 \times PBS), 100 μ l of CBX (20 mg/ml in vehicle, \sim 100 mg/kg of body weight; Sigma), or 100 μ l of glycyrrhizic acid (20 mg/ml in vehicle, \sim 100 mg/kg of body weight; Sigma). Implantation sites were detected on D4.5 [19]. If no implantation sites were detected, the uterine horns were flushed with 1 \times PBS to determine the presence of blastocysts. Another set of mice from vehicle-treated and CBX-treated groups were dissected on D7.5, and the uterine tissues were fixed in 10% formalin for histology. Two groups of pregnant females were treated with vehicle or CBX via uterine local fat pad injection [33–35] on D3 at 1800 h. Briefly, a mouse was placed on its back under anesthesia with isoflurane inhalation, and a

small incision was made in the front right side. The uterine fat pad underneath was gently pulled out (designated as the right side). Five microliters of vehicle (with blue dye to monitor the injection) or CBX (40 mg/ml in vehicle, \sim 10 mg/kg of body weight) was injected at one or two spots into the adipose tissue surrounded by uterine arteries. Implantation sites were detected on D4.5 [19]. The D4.5 uterine tissues were snap frozen and kept at -80°C . In the pseudopregnancy study, the females were mated with WT vasectomized males and randomly assigned to two groups. Artificial decidualization was induced by intrauterine oil infusion as previously described [31]. The mice were then i.p. injected with 100 μ l of vehicle or 100 μ l of CBX (20 mg/ml in vehicle, \sim 100 mg/kg of body weight) on Pseudopregnant Day 3 (D3) at 1800 h. On D4.5, artificial decidualization was detected using blue dye reaction [31]. A part of the uterine tissues was processed for transmission electron microscopy (see below), and the remaining uterine tissue was snap frozen. At least three mice were included in each group.

Transmission Electron Microscopy

Uterine segments with blue dye reaction (if present) from vehicle-treated or CBX-treated females with artificial decidualization were fixed in 2% glutaraldehyde, 2% paraformaldehyde, 0.2% picric acid, and 0.1 M cacodylate-hydrochloride buffer (pH 7.25) at 4°C for 48 h. After washing several times in 0.1 M cacodylate-hydrochloride (pH 7.25) buffer, the uterine samples were postfixed in 1% osmium tetroxide in cacodylate-hydrochloride (pH 7.25) buffer for 1 h and then washed several times in deionized water and placed in 0.5% aqueous uranyl acetate for 1 h. After several more washes in deionized water, the samples were dehydrated in an ethanol series (30%, 50%, 75%, 95%, 95%, 100%, and 100%) and cleared in acetone and propylene oxide. The samples were then infiltrated gradually with a 1:1 mixture of propylene oxide and epoxy resin before further infiltration with several changes of 100% epoxy resin. The mesometrial side of the uterine horn was trimmed off. The antimesometrial side was then orientated and embedded in a flat mold for longitudinal sections. The embedded samples were polymerized in a 65°C oven for 24 h. One-micrometer sections from the embedded blocks were obtained using an ultramicrotome (Ultracut S; Reichert) and a diamond knife (Diatome). Sections were stained with 1% toluidine blue O in 1% sodium borate and evaluated. Selected blocks were then processed for ultrathin sectioning. Thin sections of 55–60 nm were obtained and placed on grids. After poststaining with uranyl acetate and lead citrate, the grids were viewed with a transmission electron microscope (JEM-1210; JEOL USA, Inc.) at 120 keV. Images were obtained using a bottom-mount charge-coupled device camera (XR41C; Advanced Microscopy Techniques).

In Situ Hybridization

In situ hybridization was performed as previously described [31, 36]. Sense and antisense probes for *Gjb2* were synthesized from the cDNA fragment amplified with the following two primers: 1) mGjb2 e2F1, CAGCATTG GAAAGATCTGG and 2) mGjb2 e2R1, GAAGACGGCTTCAAAGATG.

Immunofluorescence and Immunohistochemistry

Immunofluorescence was performed as previously described [37] except that primary rabbit-anti-connexin 26 (1 μ g/ml; Invitrogen) antibody was used. The sections were counterstained with 0.01% 4'-diamidino-2-phenylindole dihydrochloride (Sigma). The sections from D3 WT at 2300 h and D4 at 0100 h, 0400 h, and 0600 h were also double-stained with a rat anti-integrin antibody (α 6 clone NK1-GoH3, MAB1378, 1:100 in 10% goat serum; Millipore) using red fluorescence. Immunohistochemistry for PR was performed as previously described [31].

Histology

Uterine histology was performed. The technique has been previously described [37].

Statistical Analysis

Statistical analysis of the number of implantation sites was performed using two-tailed, unequal-variance Student *t*-test. Fisher exact test was used for analyzing the implantation rates. The significance level was set at $P < 0.05$.

RESULTS

Differential Expression of Gjb2 mRNA in the Uterine LE

Microarray data (Gene Expression Omnibus number GSE44451) indicated that among the 19 gap junction proteins *Gjb2* was dramatically upregulated (14 fold) in the WT LE from preimplantation D3.5 to postimplantation D4.5 (Fig. 1A). *Gjb2* mRNA was undetectable in the preimplantation D3.5 uterus (Fig. 1B) by in situ hybridization. In the D4.5 uterus, intense *Gjb2* expression was detected in the LE at the implantation site (Fig. 1D), confirming the upregulation of *Gjb2* in the LE from D3.5 to D4.5 (Fig. 1, A, B, and D). In the D5.5 uterus, the LE had disappeared from the implantation chamber, and so had *Gjb2* signal (Fig. 1, H and I). *Gjb2* mRNA was still strongly expressed in the LE near the implantation chamber of D5.5 WT uterus (Fig. 1, F and H). It gradually disappeared in the LE away from the implantation chamber (Fig. 1, D and F).

Previously, we demonstrated that *Lpar3*^(-/-) mice had delayed implantation [19]. *Gjb2* mRNA was undetectable in the D3.5 *Lpar3*^(-/-) uterus by in situ hybridization (Fig. 1C). In the D4.5 *Lpar3*^(-/-) uterus when blue dye reaction was not obvious [19], low levels of *Gjb2* mRNA were detected in some LE cells surrounding the embryo (Fig. 1E). In the D5.5 *Lpar3*^(-/-) uterus, some LE cells still remained in the implantation chamber, and so did *Gjb2* signal (Fig. 1G). Temporal expression of *Gjb2* mRNA in the *Lpar3*^(-/-) uterus indicates its delayed upregulation parallel with delayed implantation [17]. It also indicates that the upregulation of *Gjb2* mRNA has started before embryo attachment, indicated by blue dye reaction (Fig. 1E) [32].

Upregulation of Gjb2 mRNA as a Main Mechanism of GJB2 Protein Upregulation in the LE

Multiple events (e.g., embryo attachment and decidualization) take place in the uterus from D3.5 to D4.5 [38]. How is the upregulation of *Gjb2* mRNA associated with GJB2 protein expression and uterine preparation for embryo implantation? To answer this question, the expression of *Gjb2* mRNA and GJB2 protein in serial sections from the same implantation sites of the WT uterus was examined at the very early hours of embryo implantation (D3 at 2300 h and D4 at 0100 h, 0400 h, and 0600 h) using in situ hybridization and immunofluorescence, respectively. On D3 at 2300 h when blue dye reaction was barely detectable [31], *Gjb2* mRNA was detectable in the LE at the implantation site (Fig. 2A), but GJB2 protein seemed to remain at basal level (Fig. 2B). On D4 at 0100 h, stronger expression of *Gjb2* mRNA was detected in the LE at the implantation site (Fig. 2C), and GJB2 protein was detected as small punctuated dots in the LE with some diffuse cytoplasmic staining (Fig. 2D). The upregulation of *Gjb2* mRNA continued on D4 at 0400 h in the LE at the implantation site (Fig. 2E). Upregulation of GJB2 protein, shown as an increased number of larger punctuated dots and diffuse cytoplasmic staining, was parallel with that of *Gjb2* mRNA on D4 at 0400 h (Fig. 2F). Both *Gjb2* mRNA (Fig. 2, G and I) and GJB2 protein (Fig. 2, H and J), with the latter shown as more intense and much larger punctuated dots but with less diffuse cytoplasmic staining, reached a maximum on D4 at 0600 h when decidualization became apparent [31]. On D4.5, D5.5, and D6.5, GJB2 protein was detected at the implantation chamber (D4.5 only) and surrounding LE, similar to *Gjb2* mRNA (Fig. 1, D and F, and data not shown). *Gjb2* mRNA and GJB2 protein were undetectable in the embryo from D3 at 2300 h to D6.5 (Fig. 2, A–J, and data not shown). These data demonstrate that

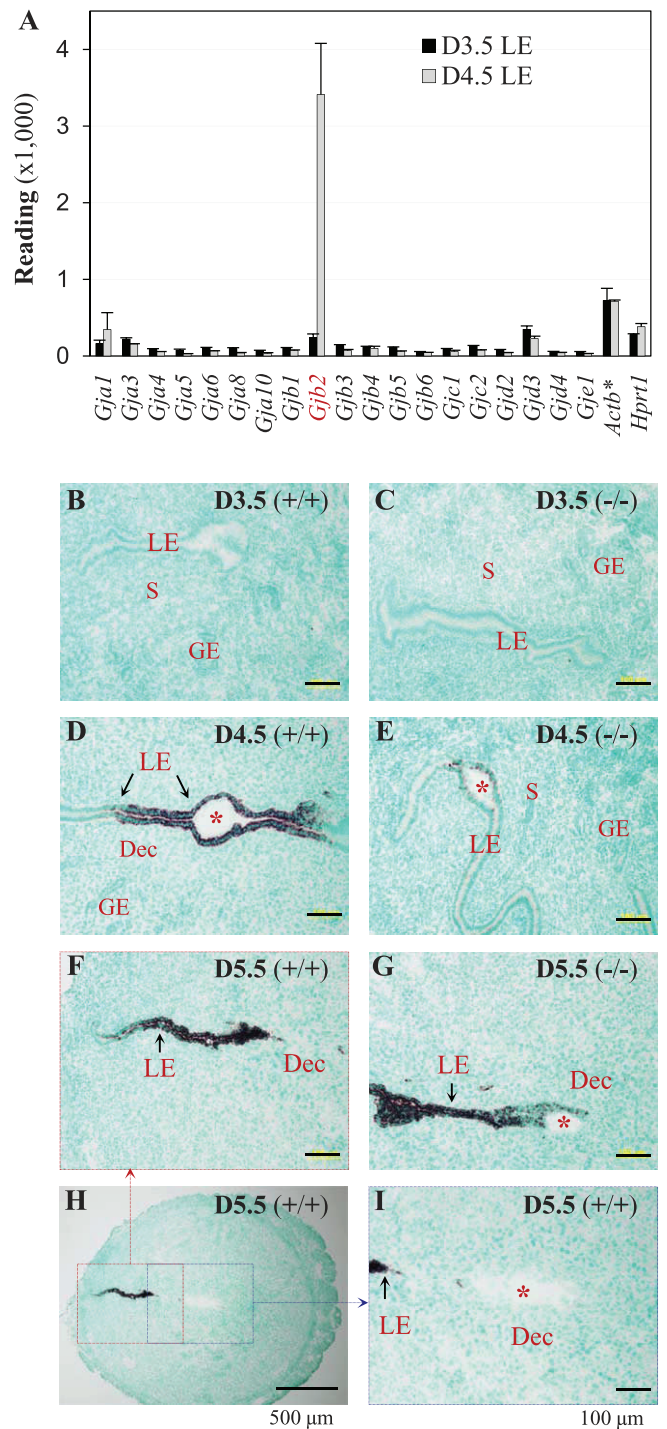


FIG. 1. Differential expression of *Gjb2* (gap junction protein, beta 2, connexin 26) mRNA in the peri-implantation mouse uterine LE. **A**) Readings of gap junction proteins from microarray analysis of D3.5 and D4.5 LE. *Actb*, β -actin, a housekeeping gene; *, one tenth of the readings; *Hprt1*, hypoxanthine phosphoribosyltransferase 1, a housekeeping gene. $n = 3$. Error bars represent SD. **B–I**) In situ hybridization of *Gjb2* in D3.5 ~ D5.5 WT (+/+) uterus and *Lpar3*-deficient (-/-) uterus with delayed implantation [19]. **B**) D3.5, +/+. **C**) D3.5, -/-. **D**) D4.5, +/+. **E**) D4.5, -/-. **F**) D5.5, +/+, enlarged view from the red box in **H**. **G**) D5.5, -/-. **H**) D5.5, +/+, low magnification ($\times 4$), the dotted red box and blue box shown in **F** and **I**, respectively. **I**) D5.5, +/+, enlarged view from the blue box in **H**. Bars = 100 μ m (**B–G** and **I**) and 500 μ m (**H**). Red star, embryo; GE, glandular epithelium; S, stroma; Dec, decidual zone.

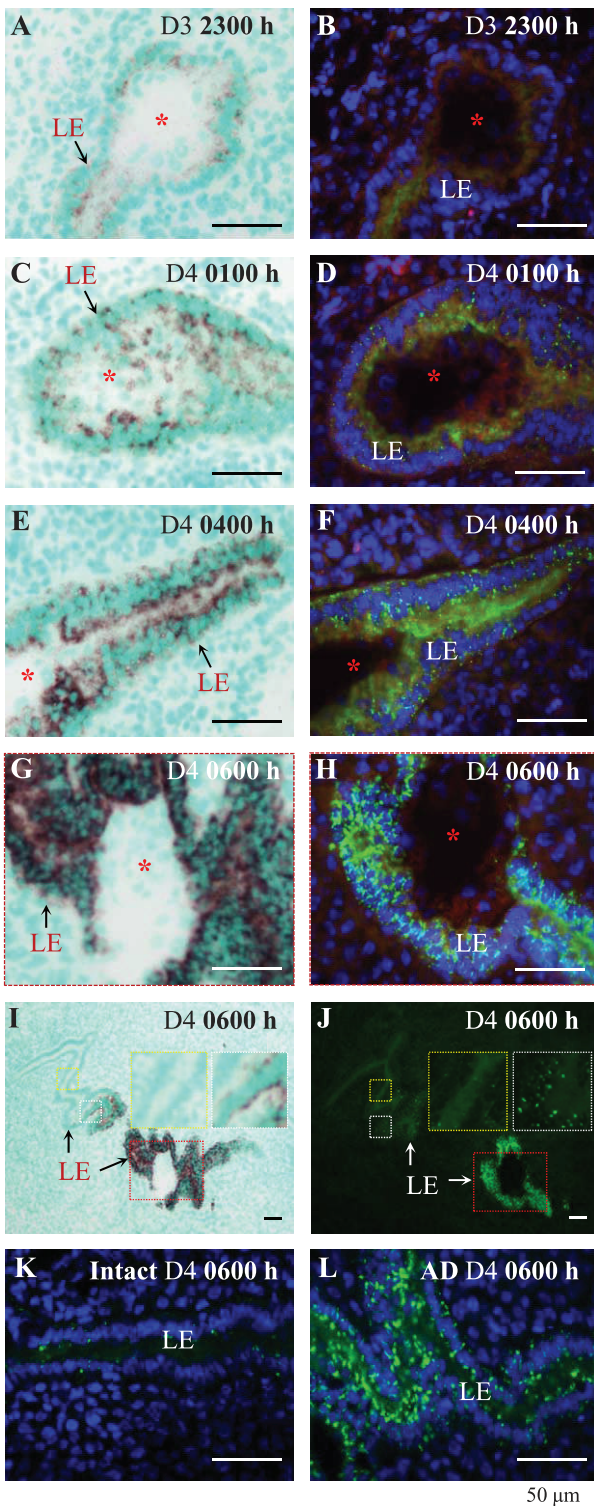


FIG. 2. Upregulation of *Cjb2* mRNA (via in situ hybridization, ISH) and GJB2 protein (via immunofluorescence, IF) in WT mouse uterine LE during early hours of embryo implantation (A–J) and GJB2 protein in the uterus with artificial decidualization (K and L). A–J) The sections for in situ hybridization and immunofluorescence at the same time point were from the same implantation sites. In situ hybridization (left panel): dark brown signal, *Cjb2* mRNA. Immunofluorescence (right panel): green, GJB2 protein; blue, 4'6-diamidino-2-phenylindole dihydrochloride; red, integrin. A) Gestation Day 3 at 2300 h, ISH. B) On D3 at 2300 h, IF. C) On D4 at 0100 h, ISH. This section likely cut through the uterine luminal epithelial cells that cover the front view of the embryo, indicated by the dark brown signals detected in the location of the embryo but no GJB2 stain on the embryo in the section from the same implantation site in D, as well as no signal of *Cjb2* or GJB2 on the embryos in A, B, and E–H. D) On

upregulation of *Gjb2* mRNA is a key mechanism for GJB2 protein upregulation in the LE, that the upregulation of *Gjb2* mRNA has already initiated when the embryo attaches to the LE, and that the dramatic upregulation of *Gjb2* mRNA happens before decidualization.

Upregulation of GJB2 in the LE by Artificial Decidualization

GJB2 was not upregulated in the D4.5 pseudopregnant uterus (data not shown) or the contralateral pseudopregnant uterine horn without oil infusion (Fig. 2K and data not shown). It was highly upregulated in the pseudopregnant uterine horn with oil-induced artificial decidualization on D4 at 0600 h (Fig. 2L) and D4.5 (data not shown), with a spatiotemporal upregulation pattern comparable to that of a pregnant uterus (Fig. 2 and data not shown), indicating that oil can serve the same role as an embryo in stimulating GJB2 expression in the LE.

Gap Junction Blocker CBX Disrupting Embryo Implantation

To determine the involvement of uterine gap junctions in embryo implantation, the broad gap junction blocker CBX was administrated via i.p. injection (100 mg/kg of body weight) to normal pregnant females on D3 at 1800 h. Implantation was detected on D4.5 and on D7.5. Among the six CBX-treated D4.5 pregnant uteri, one showed eight implantation sites (Fig. 3B), which appeared generally fainter, especially two of them, than the ones in the vehicle-treated control (Fig. 3A), indicating delayed implantation [31]. Five of the six CBX-treated pregnant females had no detectable implantation sites on D4.5 (Fig. 3, C and D), but healthy-looking hatched blastocysts were flushed from the uteri (data not shown), indicating disrupted embryo implantation. Three of these five uteri appeared shorter than the vehicle-treated control (Fig. 3D). At the same dose as CBX, glycyrrhizic acid did not affect embryo implantation detected on D4.5 (Fig. 3E). There was no significant difference in the implantation rate and the number of implantation sites between the glycyrrhizic acid-treated group and the vehicle-treated group, but the implantation rate and the number of implantation sites detected on D4.5 in the CBX-treated group were significantly lower than those in the vehicle-treated group and the glycyrrhizic acid-treated group (Fig. 3, F and G). On D7.5, all four vehicle-treated females had implantation sites (Fig. 3H), but only one of the six CBX-treated females had four implantation sites (Fig. 3I), which appeared smaller than those in the vehicle-treated group. Histology confirmed delayed embryo development at these CBX-treated implantation sites (Fig. 3M) compared with that at the vehicle-treated implantation site (Fig. 3L). The remaining five CBX-treated D7.5 uteri did not have implantation sites and had a shorter appearance (Fig. 3, J and K). Among them, one had bloody segments (Fig. 3J). Histology indicated reabsorp-

D4 at 0100 h, IF. E) On D4 at 0400 h, ISH. F) On D4 at 0400 h, IF. G) On D4 at 0600 h, ISH, enlarged view of the dotted red box in I. H) On D4 at 0600 h, IF, enlarged view of the dotted red box in J. I) On D4 at 0600 h, ISH, low magnification, the enlarged view of the dotted red box shown in G, the enlarged views of the dotted yellow box and white box shown in the two insets. J) On D4 at 0600 h, IF, low magnification, the enlarged view of the dotted red box shown in H, the enlarged views of the dotted yellow box and white box shown in the two insets. I and J) The insets showing gradient expression of *Cjb2* mRNA and GJB2 protein away from the implantation site. K) GJB2 IF, D4 at 0600 h, intact uterine horn (Intact), contralateral to the uterine horn in L. L) GJB2 IF, D4 at 0600, oil-infused uterine horn to induce artificial decidualization (AD). Red star, embryo. Bar = 50 μm.

tion of tissue protruding in the uterine lumen (Fig. 3N). Carbenoxolone treatment decreased both the implantation rate and the number of implantation sites detected on D7.5 (Fig. 3, O and P).

To further demonstrate that the CBX affected embryo implantation locally, CBX at 10 mg/kg of body weight, a dose that was one tenth of the dose for i.p. injection (Fig. 3, B, D, I, and K) but had no obvious effect on embryo implantation via i.p. injection (data not shown), was delivered via local uterine fat pad injection [33–35]. Vehicle injection did not affect embryo implantation (Fig. 3Q), while all five CBX-injected pregnant mice had local effects detected on D4.5. Three of them showed delayed implantation on the injected side only (Fig. 3R). Two of them had no implantation sites on both sides (Fig. 3S). All five CBX-treated mice had different degrees of uterine shortening on the injected side (Fig. 3, R and S). In situ hybridization of *Gjb2* on longitudinal sections crossing an embryo revealed strong expression in the LE at an implantation site from the uninjected side in Figure 3R (Fig. 3T), much lower expression in the LE at an implantation site from the CBX-injected side in Figure 3R (Fig. 3U), and no detectable signal surrounding an embryo in the uterus in Figure 3S (Fig. 3V). These results demonstrate the local effects of CBX on the uterus in disrupting embryo implantation and *Gjb2* upregulation in the LE.

Gap Junction Blocker CBX Inhibiting Artificial Decidualization

Successful implantation involves both uterus and embryo. To determine the potential effect of CBX on uterine preparation for implantation, CBX (100 mg/kg of body weight) was given via i.p. injection on D3 at 1800 h to pseudopregnant females with oil infusion in one uterine horn to induce decidualization. On D4.5, defined blue bands were detected along the oil-infused uterine horn in the vehicle-treated group (Fig. 4A). Blue dye reaction ranged from undetectable (Fig. 4B) to faint (Fig. 4C) in the oil-infused uterine horns in the CBX-treated group, which also had a shortened uterine appearance (Fig. 4, B and C). These data demonstrate the suppressive effect of the gap junction blocker CBX on artificially induced decidualization, indicating its adverse effect on uterine preparation for embryo implantation.

Gap Junction Blocker CBX Inhibiting Gap Junction Protein Expression in the LE

To determine the effect of CBX on gap junction protein expression in the LE of the above oil-infused uterine horns, GJB2 was used as an indicator. Vehicle treatment did not affect the upregulation of *Gjb2* mRNA (Fig. 4D) and GJB2 protein (Fig. 4G) in the LE, but CBX treatment prevented (Fig. 4, E and H) or suppressed (Fig. 4, F and I) the upregulation of both *Gjb2* mRNA and GJB2 protein, with the latter shown as smaller dots (Fig. 4I) than those in the vehicle-treated LE (Fig. 4G).

To correlate the inhibiting effect of CBX on gap junction protein expression in the LE, proline-rich acidic protein 1 (PRAP1) and PR were examined in serial sections. PRAP1 is upregulated in the LE [36], and PR disappears from the LE [31] upon decidualization. PRAP1 was intensely expressed in vehicle-treated LE (Fig. 4J) but was barely detectable in CBX-treated LE (Fig. 4, K and L). Progesterone receptor had disappeared in the vehicle-treated LE (Fig. 4M) but remained in the CBX-treated LE (Fig. 4, N and O). Both molecular

markers indicate no obvious decidualization in CBX-treated uteri.

Gap Junction Blocker CBX Preventing LE Preparation for Embryo Implantation

Semithin sections of the artificially decidualized uterine horns (Fig. 4, A–C) revealed a prominent uterine luminal space in the CBX-treated (Fig. 5, B and C) but not the vehicle-treated uteri, in which the apposing uterine LE cells were in tight contact with each other except at the site with an oil droplet (from oil infusion to induce artificial decidualization) (Fig. 5A). There was a thicker stromal compartment but fewer glands on the antimesometrial side, indicating decidualization, in the vehicle-treated (Fig. 5A) versus the CBX-treated uteri (Fig. 5, B and C). Figure 5C was sectioned from a uterine segment with faint blue dye reaction in Figure 4C. Endometrial edema, an event occurring between the initial blue dye reaction and decidualization [38], was seen.

Transmission electron microscopy revealed detailed LE morphology. In the vehicle-treated LE, the apical surface near the oil droplet (Fig. 5A) had irregularly shaped apical projections (Fig. 5D); apposing LE cells were tightly interdigitated in the remaining area (Fig. 5G). In contrast, the CBX-treated LE, from the most responsive situation (Fig. 4B) to the least responsive situation (Fig. 4C), had regular microvilli on the LE apical surface (Fig. 5, E and F). Although apposing LE cells in the vehicle-treated control tightly closed down upon each other, leaving no luminal space, there was a small space between the neighboring LE cells on the same side (Fig. 5G). This space was even more prominent in the area next to the oil droplet (Fig. 5A and data not shown). In the CBX-treated LE, the lateral margins of some adjacent cells had interdigitating cytoplasmic processes closing the intercellular space, while others had discernible intercellular space (Fig. 5, H and I), which was narrower than that in the vehicle-treated LE (Fig. 5G). These data demonstrate that CBX treatment inhibits the transformation of the LE to prepare for embryo implantation.

DISCUSSION

Using a pharmacological approach, this study demonstrates that gap junctions are involved in uterine preparation for embryo implantation. Spatiotemporal-specific gene knockout mice provide a good *in vivo* model to analyze the definitive *in vivo* function of an individual gap junction protein in embryo implantation. Because there are 19 gap junction proteins in mice that can form homomeric or heteromeric gap junctions and because there are potential interplays among gap junction proteins [4, 21, 26, 27], the lack of an embryo implantation phenotype in mice deficient in individual gap junction proteins such as GJA1 [22] and GJB2 (Dr. Elke Winterhager, personal communication) could not rule out the involvement of gap junctions as a functional unit in embryo implantation. Therefore, a pharmacological approach using the broad gap junction blocker CBX was a reasonable alternative strategy.

The most efficient way to deliver a drug to the uterus, especially the LE, is to inject it into the uterine lumen. However, disturbance of the uterine environment such as by intrauterine devices [39] or by excessive leakage of fluid from the fallopian tube to the uterine cavity in patients with hydrosalpinx [40] could adversely affect embryo implantation. We had examined the effect of intrauterine delivery of pharmacological compounds on embryo implantation. Unfortunately, intrauterine delivery of vehicle at various volumes

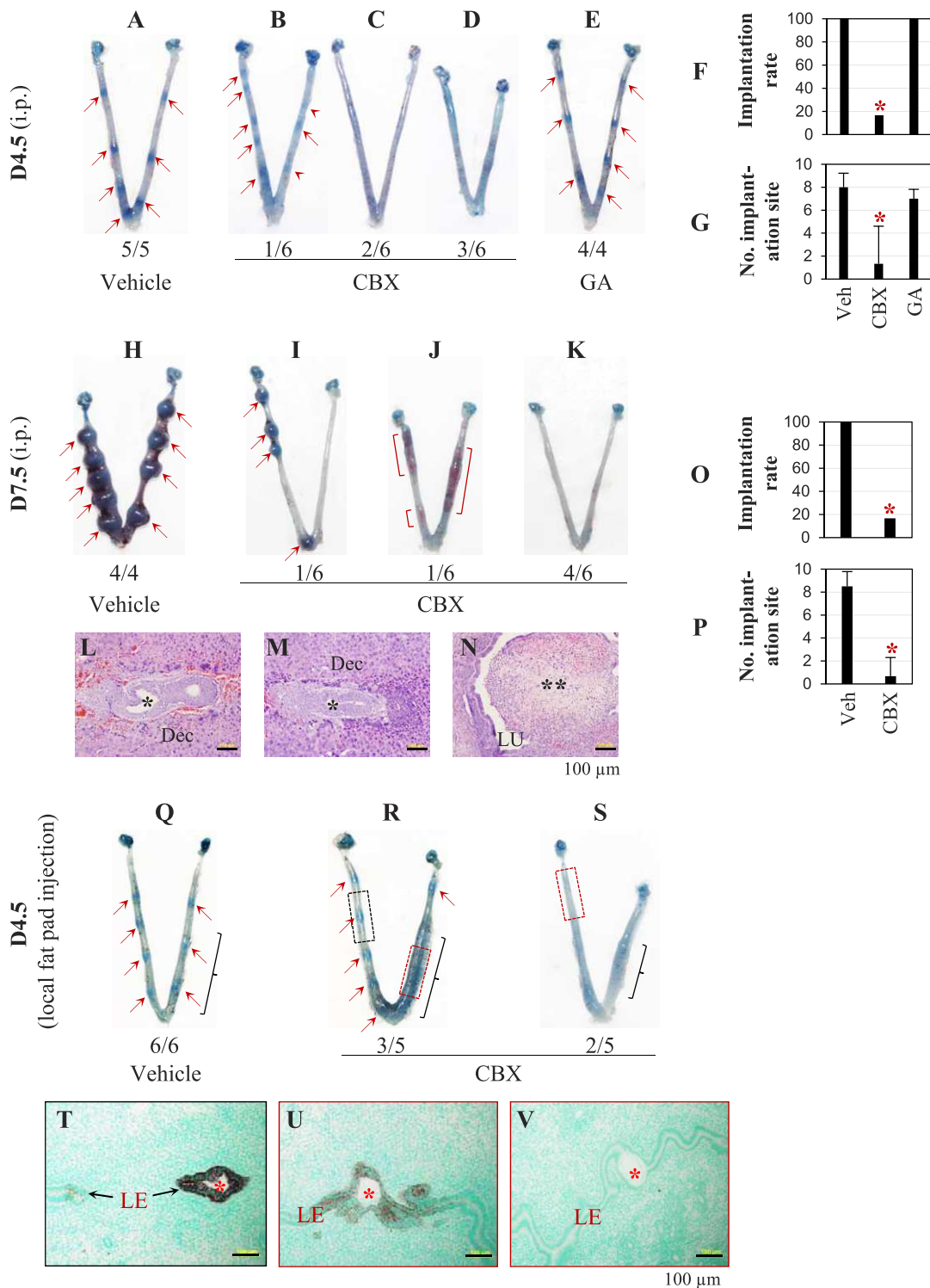


FIG. 3. Effects of CBX on embryo implantation via i.p. injection (100 mg/kg, **A–P**) and uterine fat pad injection (10 mg/kg, **Q–V**). **A–E** Uterine images from D4.5, i.p. injection. **A**) Vehicle treated. **B**) CBX treated, with six distinctive blue bands (red arrows) and two faint blue bands (red arrowheads), an indication of delayed embryo implantation. **C**) CBX treated, with no implantation and normal length. **D**) CBX treated, with no implantation and shorter appearance. **E**) Glycyrrhizic acid (GA) treated. **F**) Implantation rate on D4.5. **G**) Average number of implantation sites per mouse on D4.5. **F** and **G**) * $P < 0.05$ compared with vehicle (Veh)-treated and glycyrrhizic acid (GA)-treated groups. Error bars represent SD. $n = 4–6$. **H–K**) Uterine images from D7.5, i.p. injection. **H**) Vehicle treated, with four smaller implantation sites compared with vehicle-treated control. **I**) CBX treated, with no implantation, shorter appearance, and bloody uterine segments (red brackets). **J**) CBX treated, with no implantation and shorter appearance. **K**) CBX treated, with no implantation and shorter appearance. **L–N**) Histology from D7.5 uteri. Hematoxylin-eosin stain. Bar = 100 μ m. **L**) A section from an implantation site in **H**. **M**) A section from an implantation site in **I**. **L** and **M**) Dec, decidual zone; *, embryo. **N**) A section from a bloody segment in **J**. **, Tissue in the uterine lumen (LU) being reabsorbed. **O**) Implantation rate on D7.5. **P**) Average number of implantation sites per mouse on D7.5. **O** and **P**) * $P < 0.05$. Error bars represent SD. $n = 4–6$. **Q–S**) The D4.5 uterine images from uterine fat pad injection on the right side, with black brackets indicating the approximate locations of the injected uterine fat pad. **Q**) Vehicle injected. **R**) CBX injected, with implantation sites. **S**) CBX injected, with no implantation sites. **T–V**) Detection of *Cjb2* mRNA by in situ hybridization on longitudinal sections through an embryo in three areas indicated in **R** and **S** and processed on the same slide. *, Embryo. Bar = 100 μ m. **T**) From the black dotted rectangle in **R**. **U**) From the red dotted rectangle in **R**. **V**) From the red dotted rectangle in **S**. In **A–E**, **H–K**, and **Q** and **R**, the number

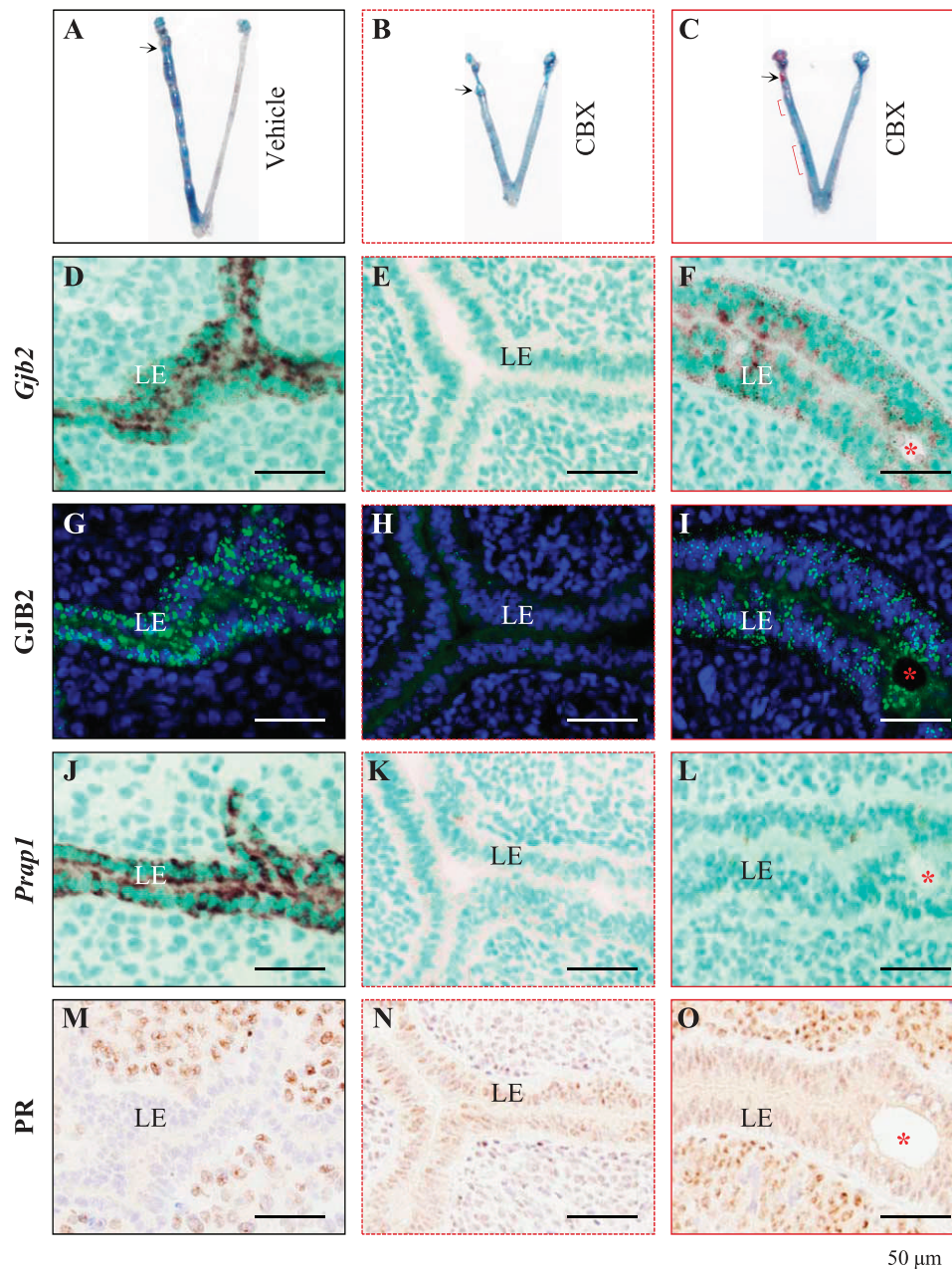


FIG. 4. Effects of CBX on artificial decidualization and uterine gene expression detected on Pseudopregnant Day 4.5. Artificial decidualization (indicated by blue segments) was induced by oil infusion of the left uterine horn of pseudopregnant mice. The injection site for oil infusion is indicated by a black arrow on uterine images in A–C. Fresh frozen longitudinal uterine sections (D–O) were cut in the orientation of mesometrial and antimesometrial. Serial sections from a blue segment (indicating decidualization) of each uterus (except B) in A–C are lined under the same column with the same outline (solid black from A, dotted red from B, solid red from C). A) Vehicle treated. B) CBX treated, representing the most suppressed decidualization upon CBX treatment, with shortened appearance. C) CBX treated, representing the least effect of CBX treatment, with shortened appearance; red bracket, suppressed decidualization. D–F) In situ hybridization detection of *Gjb2* mRNA in vehicle (D) and CBX-treated (E and F) uteri. G–I) Immunofluorescence detection of GJB2 protein in vehicle (G) and CBX-treated (H and I) uteri. J–L) In situ hybridization detection of proline-rich acidic protein 1 (PRAP1) mRNA in vehicle (J) and CBX-treated (K and L) uteri. M–O) Immunohistochemistry detection of PR protein in vehicle (M) and CBX-treated (N and O) uteri. Red star, infused oil droplet. Bar = 50 μ m.

could also disrupt embryo implantation, although to a much lesser extent than some of the pharmacological compounds tested. Uterine fat pad injection [33–35] can circumvent this issue with intraluminal drug delivery. One limitation with uterine fat pad injection in mice is the limited volume that can

be injected into the uterine fat pad, which is very small in mice.

Carbenoxolone is a broad gap junction blocker with other functions [41]. Glycyrrhizic acid shares similar structure with CBX. It has many of the same properties as CBX, including

below each uterus indicates the number of uteri (uterus) with similar appearance in the same treatment group over the total number of mice in the same group; red arrows, implantation sites.

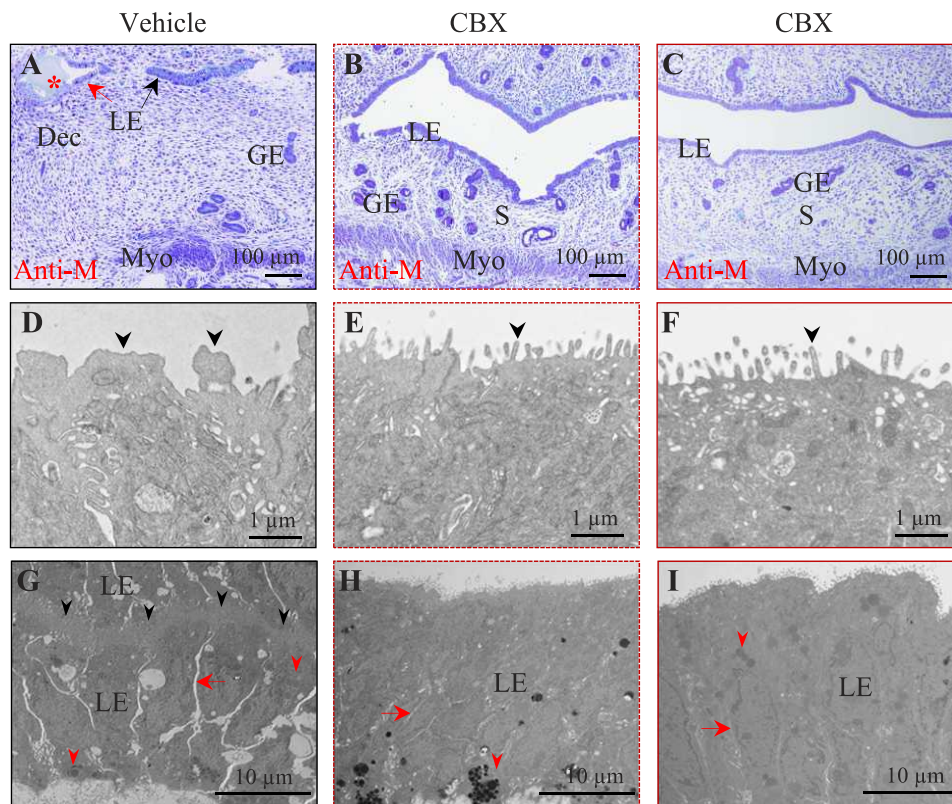


FIG. 5. Pseudopregnant Day 4.5 uterine structure of artificially decidualized uterus upon vehicle or CBX treatment. Uterine tissues were fixed for transmission electron microscopy. Solid black outlined images (A, D, and G) are from the vehicle-treated left uterine horn in Figure 4A. Dotted red line outlined images (B, E, and H) are from the CBX-treated left uterine horn in Figure 4B. Solid red line outlined images (C, F, and I) are from an area with blue dye reaction in the CBX-treated left uterine horn in Figure 4C. Longitudinal sections were cut in the orientation of mesometrial (top) and antimesometrial (Anti-M, bottom). A–C) Semithin uterine sections. A thicker stromal compartment is seen in A. Uterine lumen is open in B and C. Stromal edema is obvious in C. Red star, oil droplet. Bar = 100 μ m. D–F) Ultrastructure of the apical surface of the uterine LE. Note the irregular projections (black arrowhead) on the apical surface of the vehicle-treated LE in D, which is from the area indicated by the red arrow in A. The apical surface of the CBX-treated LE is covered by thin, regular microvilli (black arrowhead) in E and F. Bar = 1 μ m. G–I) The LE structure. Bar = 10 μ m. Red arrow, intercellular space between neighboring LE cells on the same side; red arrowhead, lipid droplet. G) The LE from the area indicated by the black arrow in A of a vehicle-treated uterus. The uterine lumen, indicated by the black arrowheads, is tightly closed by interdigitating cytoplasmic processes of the apical surface of the apposing LE cells. H) The LE from a CBX-treated uterus in B. I) The LE from a CBX-treated uterus in C. GE, glandular epithelium; S, stromal cell; Dec, decidua cell; Myo, myometrium.

anti-inflammation [28, 29], but it is ineffective in blocking gap junctions [5, 42–44]. Therefore, glycyrrhizic acid has been used as a control to determine the effect of CBX on gap junctions [5, 42–44]. Because glycyrrhizic acid had no obvious effect on embryo implantation, whereas CBX disrupted embryo implantation, it is reasonable to conclude that the effect of CBX on embryo implantation is mainly because of its effect on gap junctions. Carbenoxolone has local effects on the uterus, despite its unclear pharmacokinetics in mice. Limited data indicate that in the adult human CBX is mainly bound to plasma albumin and that the serum half-life of CBX after oral intake is about 13–16 h [45]. Carbenoxolone has been widely used in rodent models, and it has effects in different tissues [46–48]. Consistent uterine local effects such as disrupted implantation and uterine horn shortening were observed from i.p. injection and local uterine fat pad injection (one tenth of the i.p. dose) of CBX, indicating that CBX can reach the uterus.

Carbenoxolone can cause the uterus to be shorter and less stretchable. This phenomenon serves as a unique indication for the local effects of CBX on the uterus, especially via uterine fat pad injection. This observation indicates that CBX has an effect on uterine smooth muscles, which also express gap junction proteins [23], and is in line with the involvement of gap junction proteins in uterine contraction and parturition [23–

25]. The effects of CBX on embryo implantation and on uterine length seem to be independent of each other because the former mainly involves endometrium and the latter mainly involves myometrium. In addition, not all CBX-treated mice with disrupted embryo implantation had uterine shortening (Fig. 3C), and some CBX-treated nonpregnant mice (lack of embryo) had uterine shortening (data not shown).

Because embryos also express gap junction proteins [6] and embryo implantation involves both embryo and uterus, how can the effects of CBX on embryo versus uterus in embryo implantation be differentiated? To answer this question, we used an artificial decidualization mouse model, in which embryos were removed from the equation and replaced with intrauterine oil infusion to induce decidualization. Carbenoxolone treatment completely blocks or partially suppresses blue dye reaction, demonstrating that the gap junction blocker can adversely affect uterine preparation for embryo implantation. Blue dye reaction is caused by increased local capillary permeability in the stromal compartment at the implantation site upon embryo attachment to the LE [32, 49]. Because blue dye reaction became detectable about 6–8 h before decidualization became detectable [31] and because no obvious decidualization was observed in the CBX-treated uteri in the artificial decidualization model (Figs. 4 and 5), any potential

effect of CBX on decidual angiogenesis could not have had a major role on the disrupted early uterine preparation for embryo implantation initiation.

Uterine preparation for embryo implantation mainly involves the LE and stromal compartments. Because CBX is a nonspecific gap junction blocker and because there are gap junction proteins in both the LE and stromal compartments, gap junctions of which uterine compartment contribute to implantation initiation? Blue dye reaction, which becomes detectable upon embryo attachment to the LE several hours before decidualization in mice [31], can be used for our deduction. Before implantation, the expression of gap junction proteins in the uterus is suppressed [6, 11, 50]. On implantation initiation, GJB2 is dramatically upregulated in the LE before GJA1, the main gap junction protein in the stromal compartment, becomes detectable in the decidual zone (data not shown) [22]. It is expected that the major effects of CBX on gap junctions in the LE would be hours earlier than those in the decidual zone. If blue dye reaction does not occur or is faint without obvious decidualization upon CBX treatment, the effect of CBX on the LE most likely contributes to suppressed uterine preparation for implantation. Therefore, it is reasonable to conclude that gap junction proteins in the LE are involved in uterine preparation for embryo implantation. Although *Gjal*-deficient mice do not have defects in embryo implantation [22], any potential adverse effect of CBX on gap junction proteins in the stromal compartment during early hours of implantation cannot be ruled out.

What is the potential significance of gap junctions in the LE at the implantation site? One study [51] suggests that GJB2 upregulation in the LE could form a distinct communicating compartment for coordinated LE apoptosis in the implantation chamber. However, only a few apoptotic LE cells were detected at the implantation chamber on D4.5 [51, 52]. A uterine ultrastructure study [18] indicates that the loss of the LE at the implantation chamber is mainly caused by trophoblasts that interpose between the LE cells and the basal lamina to phagocytose the LE at the implantation chamber. It is possible that gap junctions in the LE of the implantation chamber may also facilitate the interposition of trophoblasts during the initial implantation process. Because gap junction proteins such as GJB2 have a negative effect on the epidermal barrier [53], it is speculated that increased gap junctions in the LE at the implantation site might be associated with disruption of the barrier (and/or increased permeability) in the LE. This may assist the reabsorption of uterine fluid during the early hours of implantation, facilitating uterine lumen closure to lock in the implanting embryo. This speculation can be supported by the observations that there is local edema at the implantation site between the initial blue dye reaction and decidualization [31, 38] and that CBX treatment prevents uterine lumen closure. The above observations also imply that gap junctions in the LE might relay the stimulus (embryo or nonembryo) from the uterine lumen to the stroma of a receptive uterus to induce decidualization.

In summary, this study demonstrates that the broad gap junction blocker CBX can disrupt uterine preparation for embryo implantation. Our findings show that uterine gap junctions are important for implantation.

ACKNOWLEDGMENT

The authors thank Dr. Zhen Fu and Dr. Shiyou Chen at the College of Veterinary Medicine, The University of Georgia, Athens, Georgia, for providing access to the imaging systems, and Dr. Elke Winterhager at the University of Essen, Essen, Germany, for sharing unpublished observations

on *Cjb2* conditional knockout mice, and Dr. Koji Yoshinaga at NICHD for advice on uterine fat pad injection.

REFERENCES

1. Willecke K, Eiberger J, Degen J, Eckardt D, Romualdi A, Guldenagel M, Deutsch U, Sohl G. Structural and functional diversity of connexin genes in the mouse and human genome. *Biol Chem* 2002; 383:725–737.
2. Maeda S, Tsukihara T. Structure of the gap junction channel and its implications for its biological functions. *Cell Mol Life Sci* 2011; 68: 1115–1129.
3. Söhl G, Willecke K. An update on connexin genes and their nomenclature in mouse and man. *Cell Commun Adhes* 2003; 10:173–180.
4. Bosco D, Haefliger JA, Meda P. Connexins: key mediators of endocrine function. *Physiol Rev* 2011; 91:1393–1445.
5. Juszczak GR, Swiergiel AH. Properties of gap junction blockers and their behavioural, cognitive and electrophysiological effects: animal and human studies. *Prog Neuropsychopharmacol Biol Psychiatry* 2009; 33:181–198.
6. Grümmer R, Reuss B, Winterhager E. Expression pattern of different gap junction connexins is related to embryo implantation. *Int J Dev Biol* 1996; 40:361–367.
7. Winterhager E, Stutenkemper R, Traub O, Beyer E, Willecke K. Expression of different connexin genes in rat uterus during decidualization and at term. *Eur J Cell Biol* 1991; 55:133–142.
8. Gabriel S, Winterhager E, Pfarrer C, Traub O, Leiser R. Modulation of connexin expression in sheep endometrium in response to pregnancy. *Placenta* 2004; 25:287–296.
9. Winterhager E, Grummer R, Mavrogianis PA, Jones CJ, Hastings JM, Fazleabas AT. Connexin expression pattern in the endometrium of baboons is influenced by hormonal changes and the presence of endometriotic lesions. *Mol Hum Reprod* 2009; 15:645–652.
10. Risek B, Gilula NB. Spatiotemporal expression of three gap junction gene products involved in fetomaternal communication during rat pregnancy. *Development* 1991; 113:165–181.
11. Grummer R, Chwalisz K, Mulholland J, Traub O, Winterhager E. Regulation of connexin26 and connexin43 expression in rat endometrium by ovarian steroid hormones. *Biol Reprod* 1994; 51:1109–1116.
12. Grummer R, Hewitt SW, Traub O, Korach KS, Winterhager E. Different regulatory pathways of endometrial connexin expression: preimplantation hormonal-mediated pathway versus embryo implantation-initiated pathway. *Biol Reprod* 2004; 71:273–281.
13. Winterhager E, Grummer R, Jahn E, Willecke K, Traub O. Spatial and temporal expression of connexin26 and connexin43 in rat endometrium during trophoblast invasion. *Dev Biol* 1993; 157:399–409.
14. Winterhager E, Brummer F, Dermietzel R, Hulser DF, Denker HW. Gap junction formation in rabbit uterine epithelium in response to embryo recognition. *Dev Biol* 1988; 126:203–211.
15. Jahn E, Classen-Linke I, Kusche M, Beier HM, Traub O, Grümmer R, Winterhager E. Expression of gap junction connexins in the human endometrium throughout the menstrual cycle. *Hum Reprod* 1995; 10: 2666–2670.
16. Wang H, Dey SK. Roadmap to embryo implantation: clues from mouse models. *Nat Rev Genet* 2006; 7:185–199.
17. Murphy CR. Uterine receptivity and the plasma membrane transformation. *Cell Res* 2004; 14:259–267.
18. Parr EL, Parr MB. Epithelial cell death during rodent embryo implantation. In: Yoshinaga K (ed.), *Blastocyst Implantation*. Rome: Serono Symposia; 1989:105–115.
19. Ye X, Hama K, Contos JJ, Anliker B, Inoue A, Skinner MK, Suzuki H, Amano T, Kennedy G, Arai H, Aoki J, Chun J. LPA3-mediated lysophosphatidic acid signalling in embryo implantation and spacing. *Nature* 2005; 435:104–108.
20. Gabriel HD, Jung D, Butzler C, Temme A, Traub O, Winterhager E, Willecke K. Transplacental uptake of glucose is decreased in embryonic lethal connexin26-deficient mice. *J Cell Biol* 1998; 140:1453–1461.
21. Ahmad S, Tang W, Chang Q, Qu Y, Hibshman J, Li Y, Sohl G, Willecke K, Chen P, Lin X. Restoration of connexin26 protein level in the cochlea completely rescues hearing in a mouse model of human connexin30-linked deafness. *Proc Natl Acad Sci U S A* 2007; 104:1337–1341.
22. Laws MJ, Taylor RN, Sidell N, DeMayo FJ, Lydon JP, Gutstein DE, Bagchi MK, Bagchi IC. Gap junction communication between uterine stromal cells plays a critical role in pregnancy-associated neovascularization and embryo survival. *Development* 2008; 135:2659–2668.
23. Tong D, Lu X, Wang HX, Plante I, Lui E, Laird DW, Bai D, Kidder GM. A dominant loss-of-function GJA1 (Cx43) mutant impairs parturition in the mouse. *Biol Reprod* 2009; 80:1099–1106.
24. Doring B, Shynlova O, Tsui P, Eckardt D, Janssen-Bienhold U, Hofmann

- F, Feil S, Feil R, Lye SJ, Willecke K. Ablation of connexin43 in uterine smooth muscle cells of the mouse causes delayed parturition. *J Cell Sci* 2006; 119:1715–1722.
25. Cluff AH, Byström B, Klimaviciute A, Dahlqvist C, Cebers G, Malmström A, Ekman-Ordeberg G. Prolonged labour associated with lower expression of syndecan 3 and connexin 43 in human uterine tissue. *Reprod Biol Endocrinol* 2006; 4:24.
 26. Liu W, Bostrom M, Kinnefors A, Rask-Andersen H. Unique expression of connexins in the human cochlea. *Hear Res* 2009; 250:55–62.
 27. Theis M, Jauch R, Zhuo L, Speidel D, Wallraff A, Döring B, Frisch C, Söhl G, Teubner B, Euwens C, Huston J, Steinhäuser C, et al. Accelerated hippocampal spreading depression and enhanced locomotory activity in mice with astrocyte-directed inactivation of connexin43. *J Neurosci* 2003; 23:766–776.
 28. Stewart PM, Whorwood CB, Walker BR. Steroid hormones and hypertension: the cortisol-cortisone shuttle. *Steroids* 1993; 58:614–620.
 29. Ming LJ, Yin AC. Therapeutic effects of glycyrrhizic acid. *Nat Prod Commun* 2013; 8:415–418.
 30. Whorwood CB, Sheppard MC, Stewart PM. Licorice inhibits 11 beta-hydroxysteroid dehydrogenase messenger ribonucleic acid levels and potentiates glucocorticoid hormone action. *Endocrinology* 1993; 132:2287–2292.
 31. Diao H, Paria BC, Xiao S, Ye X. Temporal expression pattern of progesterone receptor in the uterine luminal epithelium suggests its requirement during early events of implantation. *Fertil Steril* 2011; 95:2087–2093.
 32. Psychoyos A. New contribution to the study of the nidation of the egg in the rat [in French]. *C R Hebd Seances Acad Sci* 1960; 25:3073–3075.
 33. Yoshinaga K. Effect of local application of ovarian hormones on the delay in implantation in lactating rats. *J Reprod Fertil* 1961; 2:35–41.
 34. Ferrando G, Nalbandov AV. Relative importance of histamine and estrogen on implantation in rats. *Endocrinology* 1968; 83:933–937.
 35. Psychoyos A. New remarks on the determinism of ovum implantation [in French]. *C R Hebd Seances Acad Sci* 1962; 254:4360–4362.
 36. Diao H, Xiao S, Zhao F, Ye X. Uterine luminal epithelium-specific proline-rich acidic protein 1 (PRAP1) as a marker for successful embryo implantation. *Fertil Steril* 2010; 94:2808–2811.e1.
 37. Diao H, Aplin JD, Xiao S, Chun J, Li Z, Chen S, Ye X. Altered spatiotemporal expression of collagen types I, III, IV, and VI in Lpar3-deficient peri-implantation mouse uterus. *Biol Reprod* 2011; 84:255–265.
 38. Finn CA, McLaren A. A study of the early stages of implantation in mice. *J Reprod Fertil* 1967; 13:259–267.
 39. Makino T, Yoshinaga K, Greep RO. Effect of time of removal of intrauterine contraceptive devices on implantation and blastocyst survival in the rat. *Biol Reprod* 1971; 5:291–296.
 40. Strandell A, Lindhard A. Why does hydrosalpinx reduce fertility? the importance of hydrosalpinx fluid. *Hum Reprod* 2002; 17:1141–1145.
 41. Hanstein R, Zhao JB, Basak R, Smith DN, Zuckerman YY, Hanani M, Spray DC, Gulino M. Focal inflammation causes carbenoxolone-sensitive tactile hypersensitivity in mice. *Open Pain J* 2010; 3:123–133.
 42. Leite MC, Galland F, de Souza DF, Guerra MC, Bobermin L, Biasibetti R, Gottfried C, Goncalves CA. Gap junction inhibitors modulate S100B secretion in astrocyte cultures and acute hippocampal slices. *J Neurosci Res* 2009; 87:2439–2446.
 43. Spataro LE, Sloane EM, Milligan ED, Wieseler-Frank J, Schoeniger D, Jekich BM, Barrientos RM, Maier SF, Watkins LR. Spinal gap junctions: potential involvement in pain facilitation. *J Pain* 2004; 5:392–405.
 44. Elsen FP, Shields EJ, Roe MT, Vandam RJ, Kely JD. Carbenoxolone induced depression of rhythmogenesis in the pre-Bötzinger Complex. *BMC Neurosci* 2008; 9:46.
 45. Baron JH, Gribble JN, Rhodes C, Wright PA. Serum carbenoxolone in patients with gastric and duodenal ulcer: absorption, efficacy and side-effects. *Gut* 1978; 19:330–335.
 46. Rhee SD, Kim CH, Park JS, Jung WH, Park SB, Kim HY, Bae GH, Kim TJ, Kim KY. Carbenoxolone prevents the development of fatty liver in C57BL/6-Lep ob/ob mice via the inhibition of sterol regulatory element binding protein-1c activity and apoptosis. *Eur J Pharmacol* 2012; 691:9–18.
 47. Khorasani MZ, Hosseinzadeh SA, Vakili A. Effect of central microinjection of carbenoxolone in an experimental model of focal cerebral ischemia. *Pak J Pharm Sci* 2009; 22:349–354.
 48. Endong L, Shijie J, Sonobe Y, Di M, Hua L, Kawanokuchi J, Mizuno T, Suzumura A. The gap-junction inhibitor carbenoxolone suppresses the differentiation of Th17 cells through inhibition of IL-23 expression in antigen presenting cells. *J Neuroimmunol* 2011; 240–241:58–64.
 49. Psychoyos A. The decidual reaction is preceded by early changes in the capillary permeability of the uterus [in French]. *C R Seances Soc Biol Fil* 1960; 154:1384–1387.
 50. Grummer R, Traub O, Winterhager E. Gap junction connexin genes cx26 and cx43 are differentially regulated by ovarian steroid hormones in rat endometrium. *Endocrinology* 1999; 140:2509–2516.
 51. Joswig A, Gabriel HD, Kibschull M, Winterhager E. Apoptosis in uterine epithelium and decidua in response to implantation: evidence for two different pathways. *Reprod Biol Endocrinol* 2003; 1:44.
 52. Zhang Q, Paria BC. Importance of uterine cell death, renewal, and their hormonal regulation in hamsters that show progesterone-dependent implantation. *Endocrinology* 2006; 147:2215–2227.
 53. Djalilian AR, McGaughy D, Patel S, Seo EY, Yang C, Cheng J, Tomic M, Sinha S, Ishida-Yamamoto A, Segre JA. Connexin 26 regulates epidermal barrier and wound remodeling and promotes psoriasiform response. *J Clin Invest* 2006; 116:1243–1253.